Electronic Supplementary Material (ESI) for Catalysis Science & Technology.

Supplementary information for

Understanding the geometric and basicity effects of organic polymer modifiers on Ru/TiO$_2$ catalysts for CO$_2$ hydrogenation to hydrocarbons

Chengshuang Zhou[1] and Matteo Cargnello[1,2,*]

[1]*Department of Chemical Engineering, Stanford University, Stanford, CA 94305, USA*

[2]*SUNCAT Center for Interface Science and Catalysis, Stanford University, Stanford, CA 94305, USA*

*Corresponding author email: mcargnello@stanford.edu

This file contains additional materials and methods

1. Additional Materials and Methods

Materials

Triruthenium dodecacarbonyl ($Ru_3(CO)_{12}$, 99 %), oleylamine (OLAM, 70%), 1,4-dioxane (99%), acetic acid (99%), m-phthalaldehyde (m-PA, 99%) and $NaBH_4$ (98%) were purchased from Sigma Aldrich. 1,3,5-tris(4-aminophenyl)benzene (TAPB, 97%), 2-hydroxyisophthalaldehyde (98%), 2,6-pyridinedicarboxaldehyde (98%) were purchased from TCI. All solvents were of reagent grade and all reagents were used as-received. TiO_2 (Aeroxide, P25) was obtained from Acros and used directly as support without additional treatments. All calcined supports and samples were ground and sieved below 180 µm grain size.

Synthesis of 5 nm Ru nanoparticles

Ru nanoparticles were prepared by thermal decomposition of $Ru_3(CO)_{12}$ via colloidal synthesis using standard Schlenk techniques and following a previously reported procedure.[1] 16 mL of oleylamine (OLAM, 70%) were added to 80 mg of $Ru_3(CO)_{12}$ (99%, Sigma-Aldrich) in a three-neck flask. The reaction content was degassed (<2 Torr) for 30 min at room temperature. The flask was then flushed with nitrogen, heated to 270 °C at a rate of ~20 °C min^{-1} and kept at this temperature for 30 min. The particles were purified by precipitation with ethanol (total volume 30 ml) followed by centrifugation (8000 rpm, 3 min) and redissolution in hexanes for three times, and finally dispersed in hexanes.

Inorganic Ru/TiO_2 catalysts preparation

For the preparation of Ru/TiO_2, an appropriate amount of 5 nm Ru nanoparticles was added to TiO_2 (Aeroxide P25, Acros) support dispersed in hexanes under vigorous stirring to achieve a total metal loading of 1.0 wt. %. The mixture was stirred for 20 min to allow the nanoparticles to adsorb on the support and the catalysts were then separated by centrifugation (8000 rpm, 3 min). Colorless supernatants were observed for each solution indicating complete adsorption of the particles. The powders were dried at 80 °C for 3 h and sieved below 180 µm grain size. Organic ligands were removed by fast calcination of the catalysts at 700 °C for 30 s.

Synthesis of hybrid functional IPOP/Ru/TiO_2 catalysts

For encapsulation targeting ~10 nm overlayer thickness, 500 mg of Ru/TiO_2 catalysts together with 1.08 mmol of phthalaldehyde (either m-, OH- or py-) were added into 30 ml of 1,4-dioxane and sonicated for 20 mins until full dispersion/dissolution. 250 mg of 1,3,5-tris(4-aminophenyl)benzene (TAPB, 97%, TCI) was separately dissolved in 30 mL 1,4-dioxane. The two solutions were then mixed and vigorously stirred for 30 mins at room temperature to promote adsorption of organic monomers onto inorganic substrates. 4 mL of acetic acid was then added as Brønsted acid catalyst for imine condensation. The polymerization was allowed to proceed for 90 mins, after which products were collected by centrifugation and subsequently washed with THF and acetone. The samples were finally dried at 80 °C under dynamic vacuum conditions for 12 h.

Conversion of hybrid py-IPOP/Ru/TiO_2 to py-APOP/Ru/TiO_2 catalyst

300 mg of py-IPOP/Ru/TiO_2 were added to a 100 ml flask together with 45 ml of 1,4-dioxane. Under vigorous stirring, 1.5 g of $NaBH_4$ was added in small portions. The mixture was continuously stirred for 6 hrs. After the addition of 6 ml of methanol, the mixture was allowed to react for another 12 hrs under stirring. The reaction was quenched with H_2O, after which products

were collected by centrifugation and subsequently washed with THF and acetone. The samples were finally dried at 80 °C under dynamic vacuum conditions for 12 h.

Catalyst characterization

Thermogravimetric analysis (TGA) was performed on a TA Instruments TGA-500. Samples were heated at a ramp rate of 5 °C min^{-1} under a flow of 25 mL min^{-1} of air.

Bright-field transmission electron microscopy (TEM) was performed on a FEI G2 F20 X-TWIN Transmission Electron Microscope operating at 200 kV. The thickness of the organic overlayers were determined from TEM measurements.

X-ray photoelectron spectroscopy (XPS) was performed using a PHI VersaProbe 3 Scanning XPS Microprobe equipped with a hemispherical electron analyser using Al(Kα) radiation (1486.3 eV). For all samples, the incident X-ray spot size was 100 um, and an excitation of 100 W at 20 kV was applied. An Ar^+ neutralizer and electron flood gun were used to compensate for sample charging. Binding energies were referenced to the C 1s peak (284.8 eV).

Gas adsorption measurements were carried out in a Micromeritics 3-Flex instrument, which uses high-accuracy pressure transducers to measure gas adsorption. For N_2 physisorption experiments, samples were degassed in the Micromeritics SmartVacPrep unit below 0.1 Torr for 19 h at 150 °C, with masses measured after degassing. N_2 isotherm was then measured in 12 mm borosilicate tubes containing ~100 mg of powder samples, in a bath of liquid nitrogen.

The amount of exposed Ru sites were determined from CO chemisorption experiments, where ~150 mg of catalyst powder was loaded in a quartz tube and subjected to pretreatments consisting evacuation at 110 °C for 30 min, oxidation in O_2(5 vol %)/Ar at 250 °C for 30 min, further evacuation at 250 °C for 30 min, and reduction in H_2(5 vol %)/Ar at 250 °C for 30 min followed by evacuation at 250 °C for 2 h and 180 °C for 6 h. The CO adsorption experiments were conducted at −70 °C to avoid the formation of carbonates on TiO_2 using an ethanol/dry ice bath and in the pressure range from 2 to 20 Torr.

Fourier Transform Infrared Spectroscopy (FTIR) measurements of the samples were performed on a Thermo-Fisher Nicolet is-50 FTIR instrument with an attenuated total reflectance attachment using a deuterated triglycine sulfate detector with 2 cm^{-1} precision.

Catalytic measurements

Catalytic experiments were conducted in a custom-made stainless-steel reactor with an internal diameter of 1 cm. Approximately 40 mg of Ru/TiO_2 or 100 mg of encapsulated catalysts were physically mixed with SiC to reach a total mass of 300 mg and loaded into the reactor in between two layers of granular acid-washed quartz. Prior to reaction, the catalysts were activated by oxidation at 250 °C in 5% O_2/Ar atmosphere for 30 minutes and subsequent reduction at 250 °C in 5% H_2/Ar atmosphere for another 30 minutes. After pretreatments, the reactant gas mixture (75% H_2 + 25% CO_2) was fed into the reactor at the flow rate of 30 mL min^{-1}. The total pressure of the reactor was gradually raised to 2, 4, 6, 8 and 10 bar, and reactivity data was collected for 3 hrs at each pressure level. All products remained in the gaseous phase and thus continuously analyzed by a GC system equipped with a Hayesep D column and a molecular sieve 5A column. CO and all hydrocarbons were quantified using flame ionization detector (FID), while H_2 and CO_2 consumption was measured using thermal conductivity detector (TCD).

CO_2 conversion was calculated by the equation:

$$CO_2\ conversion\ (\%) = \frac{CO_{2_{in}} - CO_{2_{out}}}{CO_{2_{in}}} \cdot 100\%$$

Where CO_2 (in) and CO_2 (out) denote moles of CO_2 at the inlet and outlet, respectively.

Selectivity distribution of individual products was calculated by equation:

$$C_xH_y\ Selectivity\ (\%) = \frac{x \cdot C_xH_y}{CO_{2_{in}} - CO_{2_{out}}} \cdot 100\%$$

Where $C_xH_yO_z$ denote moles of possible products, such as CO, CH_4 and other hydrocarbons in the outlet.

Turnover frequency of individual products was calculated by equation:

$$C_xH_y\ rate\ (\mathrm{\mu mol \cdot g_{\mathit{Ru}}{}^{-1} \cdot s^{-1}}) = \frac{CO_2\ flow\ rate\ (\mathrm{\mu mol \cdot g^{-1} \cdot s^{-1}}) \cdot yield\ of\ C_xH_y(\%) \cdot x}{total\ amount\ of\ Ru\ per\ sample\ weight\ (\mathrm{g \cdot g^{-1}})}$$

$$C_xH_y\ TOF\ (\mathrm{s^{-1}}) = \frac{N_A\ (\# \cdot \mathrm{mol^{-1}}) \cdot CO_2\ flow\ rate\ (\mathrm{mol \cdot g^{-1} \cdot s^{-1}}) \cdot yield\ of\ C_xH_y(\%) \cdot x}{number\ of\ exposed\ Ru\ sites\ per\ sample\ weight\ (\# \cdot \mathrm{g^{-1}})}$$

Calculation of C-C coupling probability (α)

Generally, hydrocarbon production from CO_2 hydrogenation on Ru catalysts share similar mechanism with Fischer-Tropsch synthesis and thus follows Anderson–Schulz–Flory (ASF) distribution because of the polymerization nature of the process. Specifically, the molar percentage of a hydrocarbon product with carbon number n (M_n) is dependent on the C-C coupling probability α ($0 < \alpha < 1$) by the following equation:

$$M_n = (1 - \alpha)\alpha^{n-1}$$

In order to obtain the value of α from experimental data, the above equation is often expressed in the logarithmic form and fitted linearly ($\ln(M_n)$ vs n) to get the slope, which equals to $\ln(\alpha)$, as described below:

$$\ln(M_n) = nln(\alpha) + \ln\left(\frac{1-\alpha}{\alpha}\right)$$

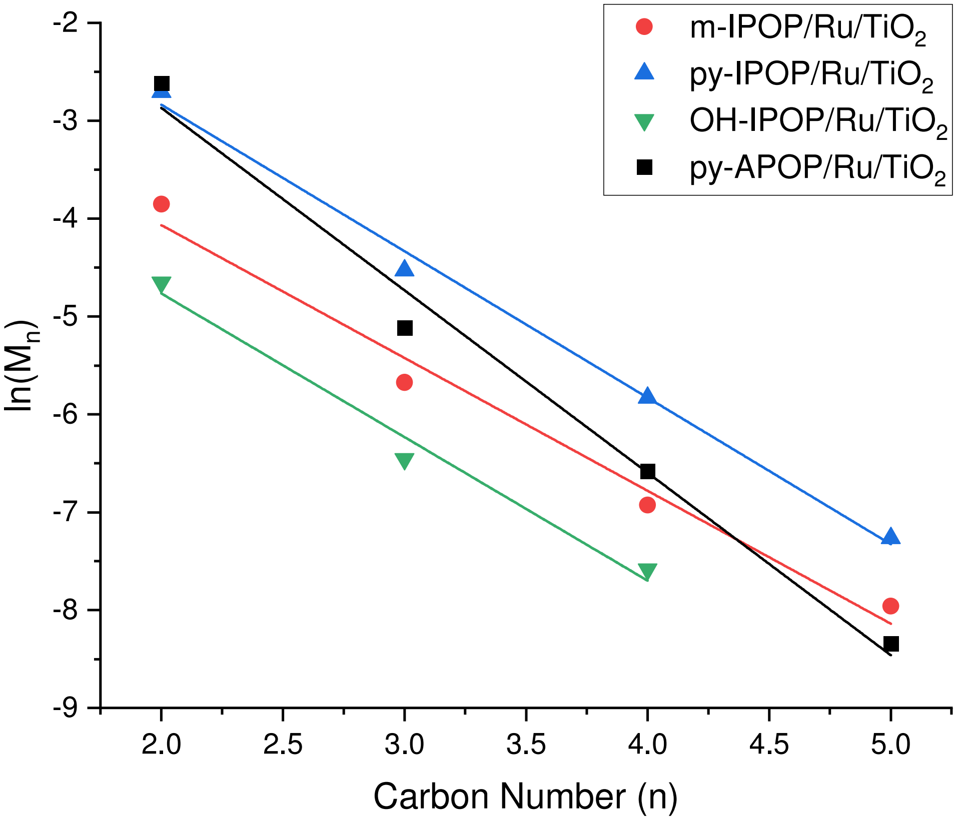

-2
-3
-4
-5
-6
-7
-8
-9
ln(M$_n$)
2.0
2.5
3.0
3.5
4.0
4.5
5.0
Carbon Number (n)
● m-IPOP/Ru/TiO$_2$
▲ py-IPOP/Ru/TiO$_2$
▼ OH-IPOP/Ru/TiO$_2$
■ py-APOP/Ru/TiO$_2$

Sample	**Chemisorption Area ($m^2_{metal} \cdot g^{-1}_{catalyst}$)**
Ru/TiO_2	1.58
m-IPOP/Ru/TiO_2	0.15
py-IPOP/Ru/TiO_2	0.07
OH-IPOP/Ru/TiO_2	0.14
py-APOP/Ru/TiO_2	0.08

Table S1. CO chemisorption results of the catalysts

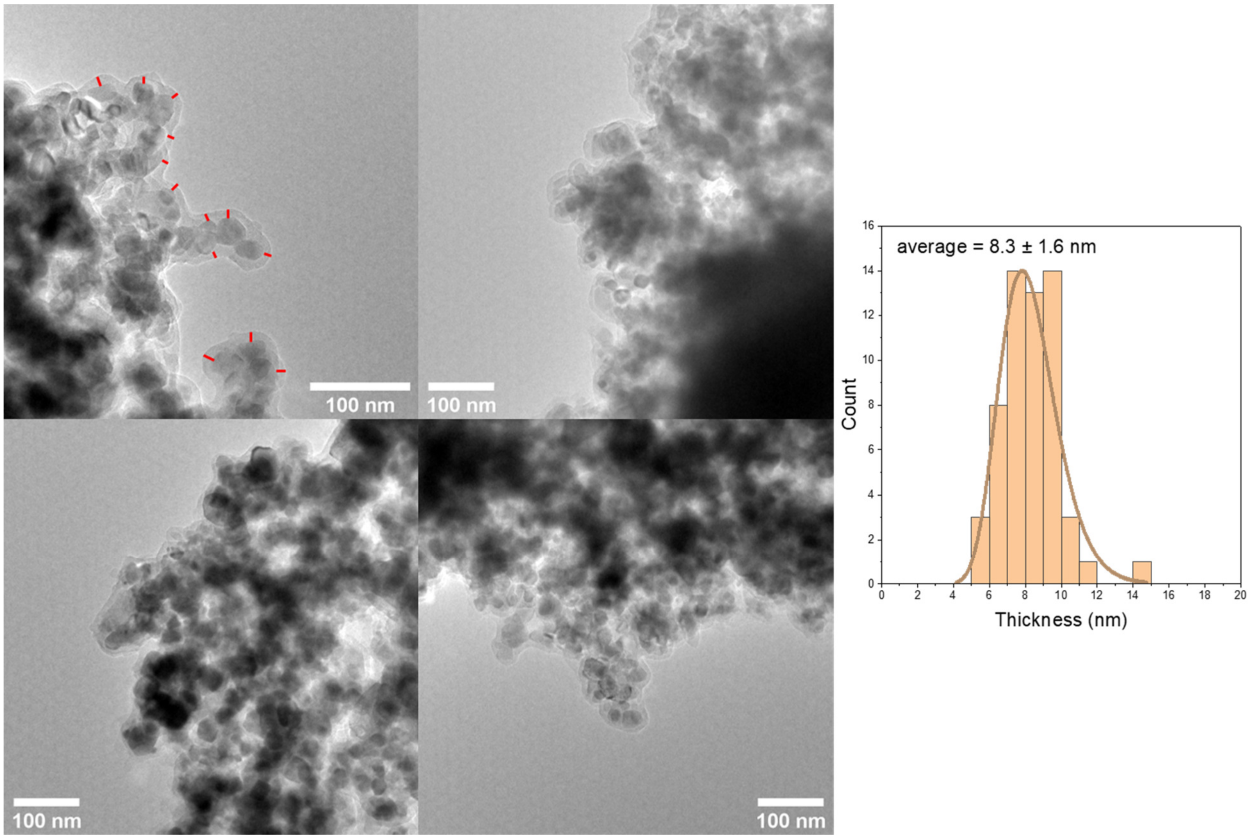

Fig. S1. Additional TEM images of m-IPOP/Ru/TiO_2 that were used for overlayer thickness measurements. Red lines were examples showing where the measurement was made. Specifically, wherever an individual TiO_2 particle could be identified, a vertical line was drawn from the TiO_2 external surface to the closest perimeter of the organic overlayer. Only one line was drawn from each TiO_2 particle, and the average length of the lines was used as the average thickness of the organic overlayer.

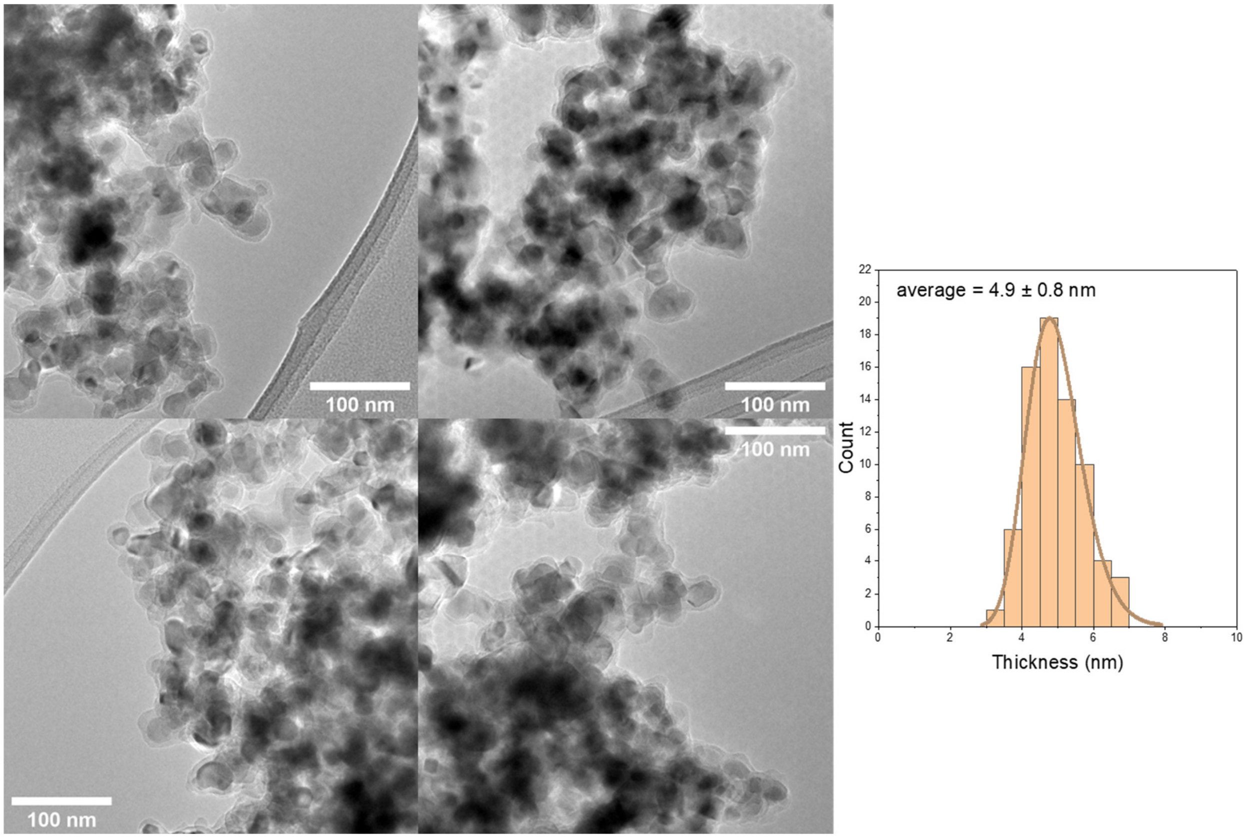

Fig. S2. Additional TEM images of py-IPOP/Ru/TiO$_2$ that were used for overlayer thickness measurements.

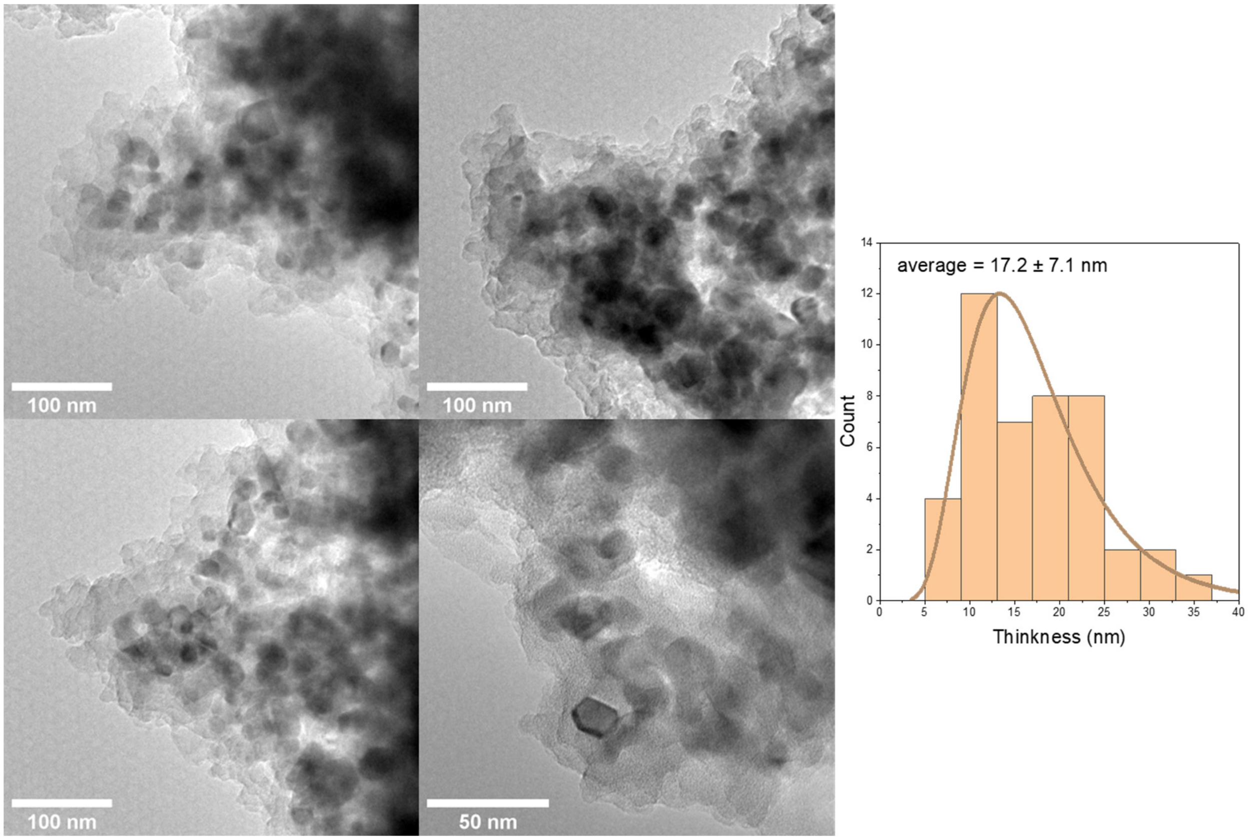

Fig. S3. Additional TEM images of OH-IPOP/Ru/TiO_2 that were used for overlayer thickness measurements.

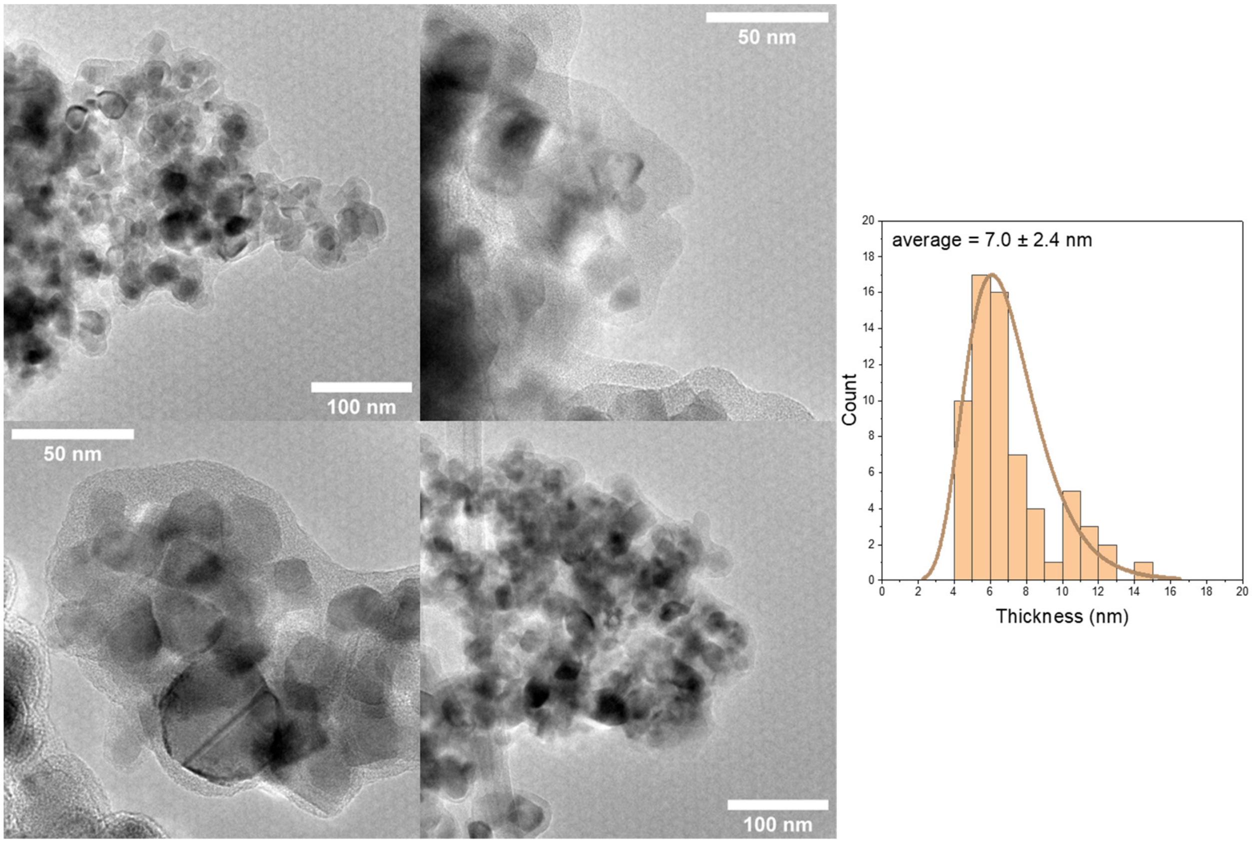

Fig. S4. Additional TEM images of py-APOP/Ru/TiO_2 that were used for overlayer thickness measurements.

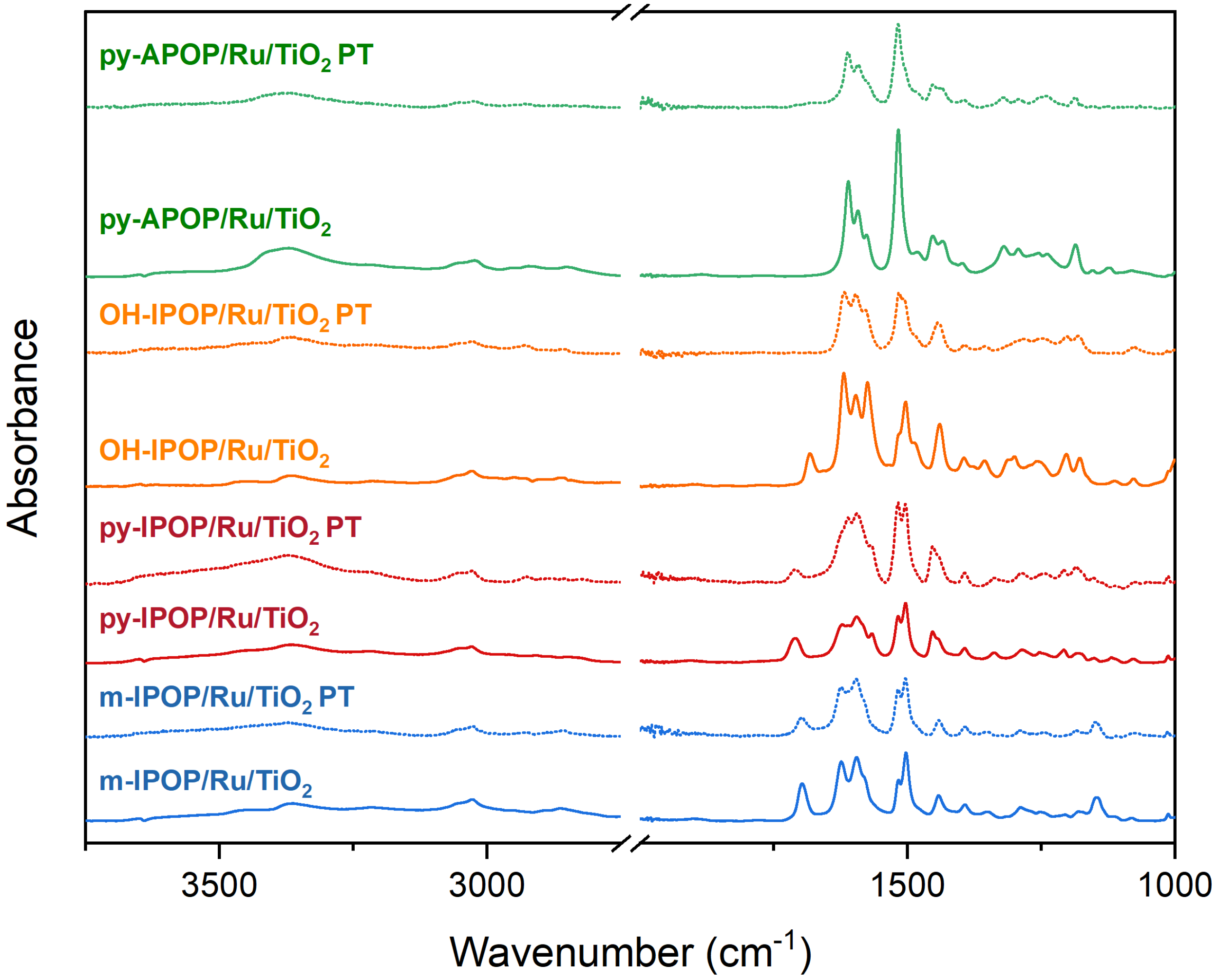

Fig. S5. Attenuated Total Reflectance Infrared spectra of the catalysts prepared in this work, before and after CO_2 hydrogenation reaction at 250 ºC, 30 sccm 3:1 H_2:CO_2, 10 bar. PT denotes “post-test”.

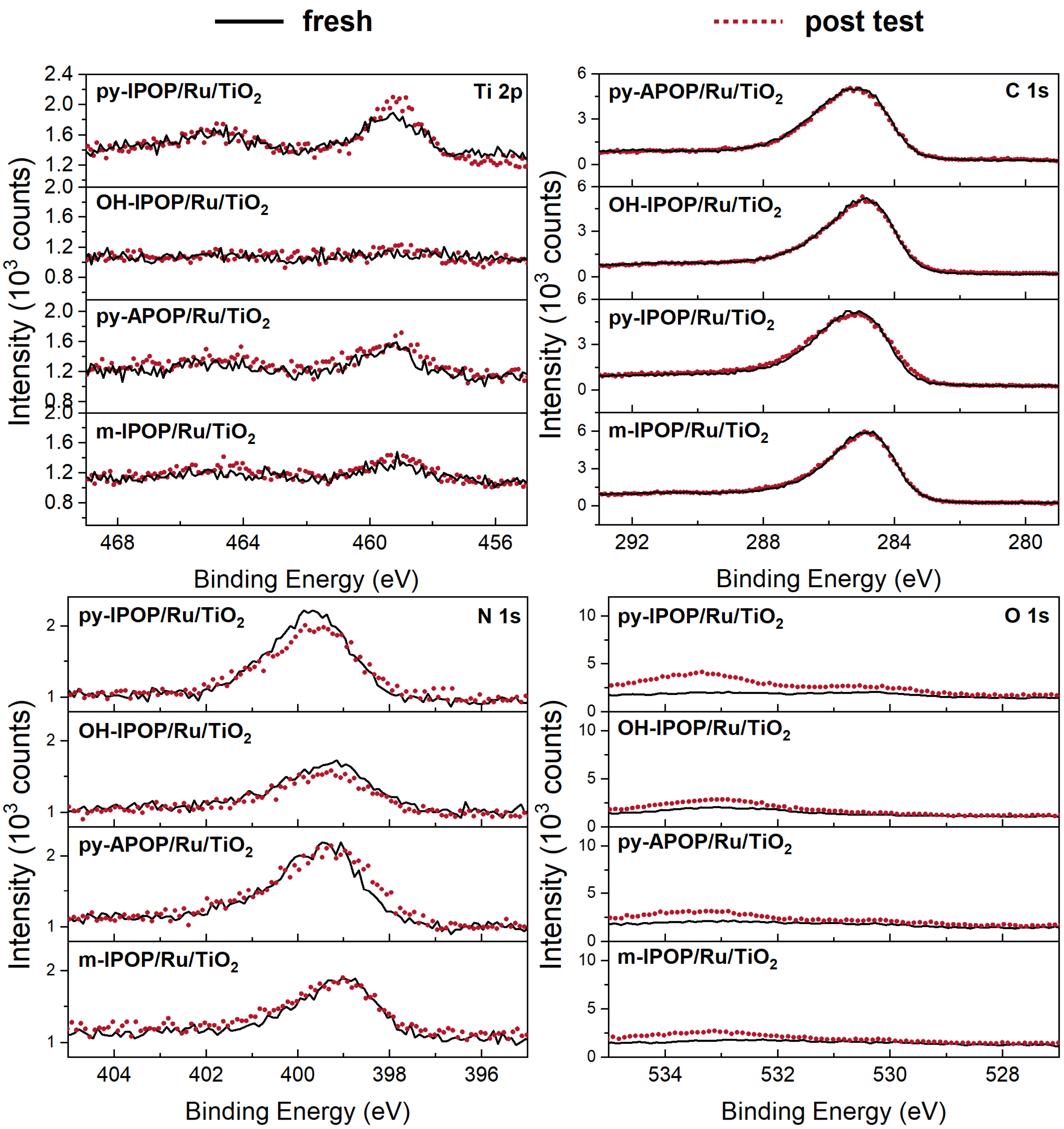

Fig. S6. XPS analysis of the catalysts before and after CO_2 hydrogenation reaction at 250 ºC, 30 sccm 3:1 H_2:CO_2, 10 bar. Black solid lines represent as-synthesized catalysts and red dots represent post-test catalysts. Increase in oxygen 1s peak at ~533 eV were attributed to adventitious oxygen from slightly oxidized SiC, which was used as diluent during catalysis tests.

References

1. A. Aitbekova, E. D. Goodman, L. Wu, A. Boubnov, A. S. Hoffman, A. Genc, H. Cheng, L. Casalena, S. R. Bare, M. Cargnello, Angew. Chem. Int. Ed. 2019, 58, 17451.